ON THE POLYMER PLASMA LASER ABLATION

Maria-Alexandra PAUN[1],
Vladimir-Alexandru PAUN[2], Viorel-Puiu PAUN[3]

Rezumat. *Plasma polimerică determinată prin procedura de ablație cu laser a fost examinată experimental. Dinamica penei de plasmă a fost ilustrată cu succes in articol. Rezultatele investigatiei sunt în excelent acord cu cele cunoscute din lucrările publicate în domeniu.*

Abstract. *The polymeric plasma determined by the laser ablation procedure was experimentally examined. The dynamics of the plasma plume have been successfully illustrated in paper. The results of the investigation are in excellent agreement with those known from the works published in the field.*

Keywords: polymer; plasma; laser ablation; plasma plume

DOI https://doi.org/10.56082/annalsarsciphyschem.2022.1.99

1. Introduction

In physics, plasma is a well-defined state of matter aggregation, consisting of ions, electrons, and neutral particles (atoms or molecules), considered generically neutral. In the sense of the first definition, plasma can be considered as a total or partially ionized gas, but on the whole neutral from an electrical point of view. However, it is seen as a distinct state of aggregation, more precisely the fourth state, having specific properties in this respect [1]. The plasma temperature obtained in the laboratory may take different values for each type of constituent particle. In addition, the spontaneous ignition of plasma depends on many parameters (concentration, external electric field, etc.), being impossible to establish a temperature at which the passage of matter takes place, from gaseous state to plasma itself.

In the established definition, laser ablation or photoablation (as it is also called) is a physical process of removing material from a solid (or occasionally liquid) aggregation states surface by irradiating it with a laser beam power, considered to be the decisive factor in the penetration of material.

[1]PhD, School of Engineering, Swiss Federal Institute of Technology (EPFL), 1015 Lausanne, Switzerland; (e-mail: maria_paun2003@yahoo.com).
[2]PhD, Five Rescue Research Laboratory, 75004 Paris, France, (e-mail: vladimir.alexandru.paun@ieee.org) .
[3]Prof., Department of Physics, Faculty of Applied Sciences, University Politehnica of Bucharest, 060042 Bucharest, Romania, corresponding member of Academy of Romanian Scientists, (e-mail: viorel.paun@physics.pub.ro).

Historically speaking, the first laser ablation experiments using the polymers as practical targets were published by Srinivasan and Mayne-Banton in year 1982 [2]. In that period, laser ablation of polymers was considered as an alternative to the conventional photoresist technology, the only one recognized up to that time. This method never reached the breakthrough in industry due to the high ablation thresholds and the redeposition of the ablated material (debris). Since then, other major applications have been detailed with great success and are now applied in the productive companies [3]. Nowadays, the laser ablation of polymers is a smart procedure to directly produce 3D structures, respectively spatial objects [4].

The current paper is founded on four distinct chapters. The first chapter presents the introductory notions of plasma physics, along with the technical definition of laser ablation. The next chapter, the second, is devoted to the experimental technique used, as the title suggests. The third chapter, entitled Results and discussion, starts with introducing the experimental results, analyses the various compartmental aspects, including plasma expansion, temporal ion current oscillation, as well as the two-dimensional time and position in temperature evolution. In the last section, section four, the conclusions are synthetically presented.

2. Experimental technique

In this subsection we will talk about the experimental technique used. The investigational device is established on a structure, which was initially used for analytical scope and described with detail in articles [5, 6].

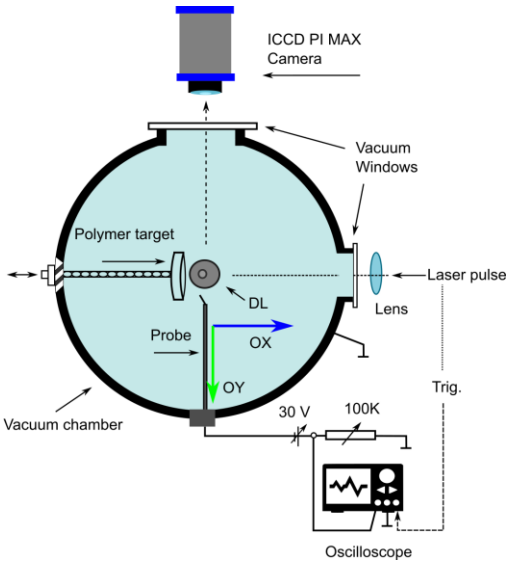

Fig. 1. The experimental installation presentation/show

The Figure 1 shows the vacuum chamber and the localization of the polymer target and the probe, together with the laser pulse and the oscilloscope.

The tests have been effectuated in a vacuum chamber, built entirely of stainless steel, and rapidly ejected by ability of a 450 l/s turbomolecular automatic pump, to a base pressure smaller than 10-6 torr (p < 10-6 Torr). As a necessary maneuver for the experimental process, it is then intervened by 10 ns Nd:YAG laser, and pulsed laser beam (with the wavelength, λ = 532 nm), which is focused by a lens with focal radius f = 25 cm on the polymer target (the polymer composition will be presented in continuation of the paragraph) placed in the same enclosure, respectively the vacuum chamber. The rough spot diameter at the striking/impact point has been around 300 μm (~300 μm) [6].

The beam energy of laser used (somewhere in between 1-100 mJ/pulse) has been constantly monitored by a standardized high-resolution device called OPHIR joulemeter. The energy usually employed was ~40 mJ/ pulse, this leads to a typical laser intensity of ~5.7 GW/cm^2.

In the present study, we used a thin diblock copolymer, polystyrene-block-poly(4-vinylpyridine) (PS-b-P4VP), film doped selectively with tetrakis(4-carboxyphenyl) porphine (TCPP) into the nanoscale spherical domains of P4VP as a target polymer film.

3. Results and discussion

The plasma expansion is analyzed in a system of plane and normalized coordinates in the region above the target. The *Oy* axis coincides with the symmetry axes of the laser pulse, and the *Ox* axis is considered along the target surface.

Also, the experimental results of a diblock copolymer film used as target in a Nd: YAG laser (λ = 532 nm) ablation process, were analyzed. A good correlation between the experimental data and the theoretical model was highlighted [4].

According with our experimental data, the amplitude exponential decay factor is $\delta(t) = (4.16 \pm 0.34) MHz$ (obviously being a frequency, 1Hz= s^{-1}), the oscillations period is $T = 1/\delta(t) = 240\, ns$ and the velocity of the polymer plasma plume is $v = \sqrt{4\pi\alpha\delta(t)} \approx 5 \cdot 10^4\, m/s$ for $\alpha = 46\, m^2/s$ (for details of α value see [7, 8]).

In Figure 2, the temporal ion current oscillation of plasma structure is shown. A good behavior (almost identical) on the t ≤ 1.2 10^{-6}s interval, then in the rest of the time range, is observed. With blue color, tending asymptotically to zero, visible on the graph, the corresponding asymptote is drawn.

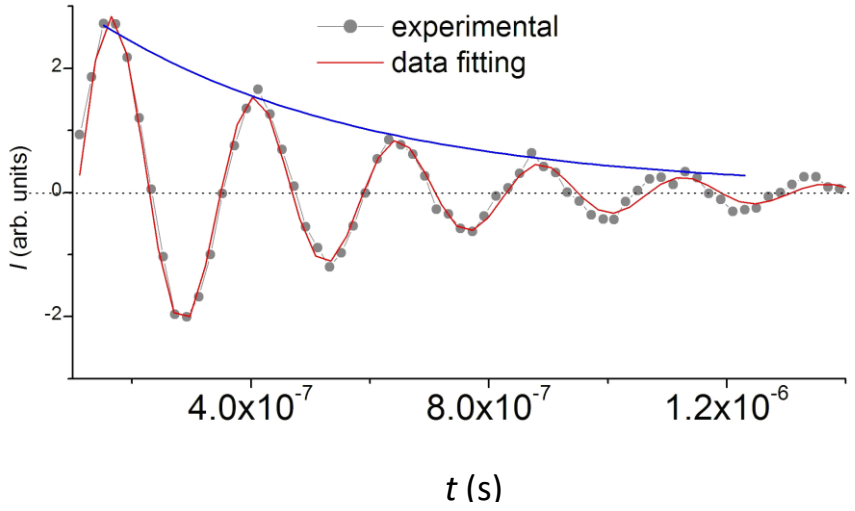

Fig. 2. The temporal ion current oscillations

In Figure 3, the estimation of temperature versus x, position in the probe, and time t, is shown [9]. This is the graphic representation of complete solution for the temperature distribution in a two-dimensional case. An initial condition associated with the modeling of heat flow in a geometrical structure is written as u(x, 0) = f(x) where f(x) is a prescribed initial temperature distribution over the probe. The Dirichlet boundary conditions for the strictly 2D geometry would be to specify the temperature at the ends of the structure and are written u(0, t) = T_0 and u(L, t) = T_1, where T_0 and T_1 are specified temperatures. The complete solution for the temperature distribution and all graphic representations were obtained using the finite differences method [10, 11].

In the 2D graphs, the depth of temperature is specified by a colormap bar.

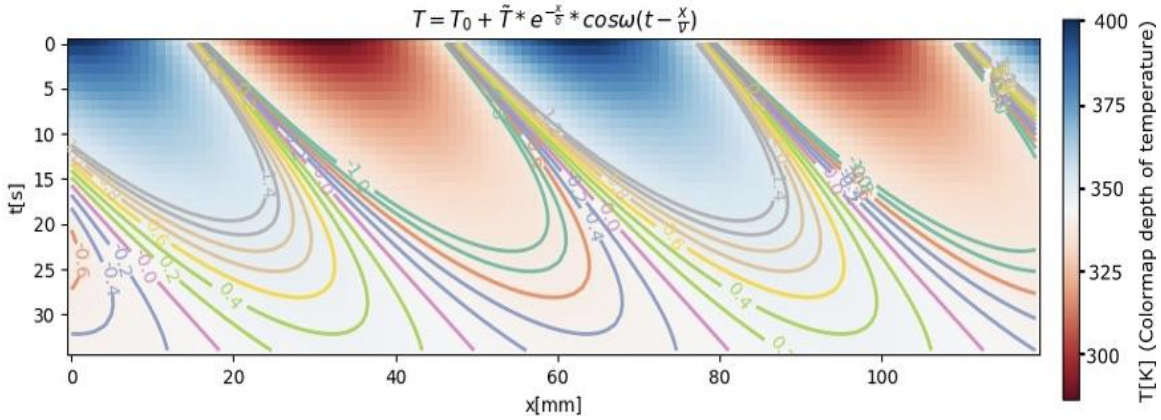

Fig. 3. 2D time and position evolution of temperature. Application in colormap depth of temperature

In Figure 4, the estimation of temperature function of t (time) and x (position in the probe) is presented. In the 3D graphs, the value of temperature is specified by a colormap bar [9].

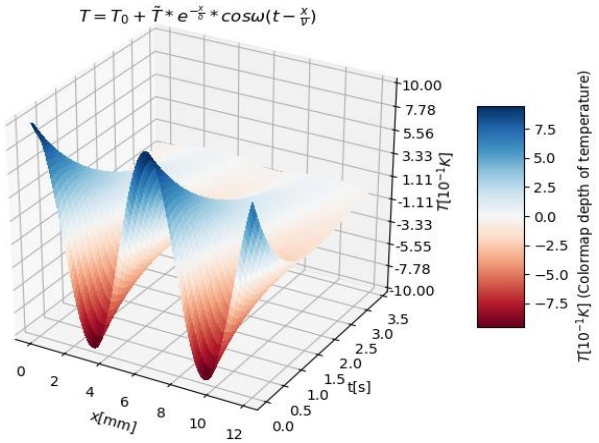

Fig. 4. The 3D graphs of temperature versus time and position

In Figure 5, the evolution of the visible emission from the polymer plasma plume recorded using an ICCD PI MAX camera (gating time 20 ns) is listed. Successive laser pulses of equal energy (40 mJ/pulse) were used to record the different shots, for 400 ns, 600 ns, 800 ns, 1000 ns, respectively 1200 ns.

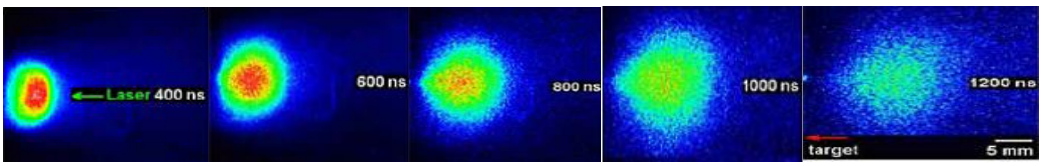

Fig. 5. Evolution of the visible emission from the polymer plasma plume

In the chained figures, one after the other, it is observed a longer evolution time wherein the plume aspect is more attenuated, and the emission is poor. Subsequent of their recording, the images are communicated to the computer where they can be extra investigated.

In order to appreciate the expansion velocities, 2-dimensional images namely “snapshots” of the laser determined plasmas were registered at constant laser fluence (19 J/cm^2) at different moments in time with respect to the laser beam. During the expansion, the LPP enlarges its volume and the point named center-of-mass, assessed as the maximum emission intensity zone, shifts to upper distances

as the registration time is modified. This determines the conclusion that the expansion velocity is a constant value over the total lifetime of the plume structure.

Benefiting of advanced optical analysis procedures, the speed of the plasma plume structure is simply estimated by dividing the distance of the maximum plasma emissivity position to the time corresponding to its obtaining. Experimental data are represented graphically in Figure 5. The measurements performed could be interpreted and solved through simple linear regression without the intercept term (single regressor) and the plume formation speed can be evaluated. By a final calculation, we achieved a value of $v_1=4.66\cdot10^4$ m/s for plume pattern displacement, Figure 6.

A fact observed, respectively in the evolution of the visible emission from the polymer plasma feathers, which refers to the differentiation into two types of plasma structures on the last three photographs, those taken at 800, 1000 and 1200 ns, is shown in Figure 6. More precisely, the differentiation in two distinct plasmatic structures is distinguished, with the highlighting of one that lags behind, having another speed.

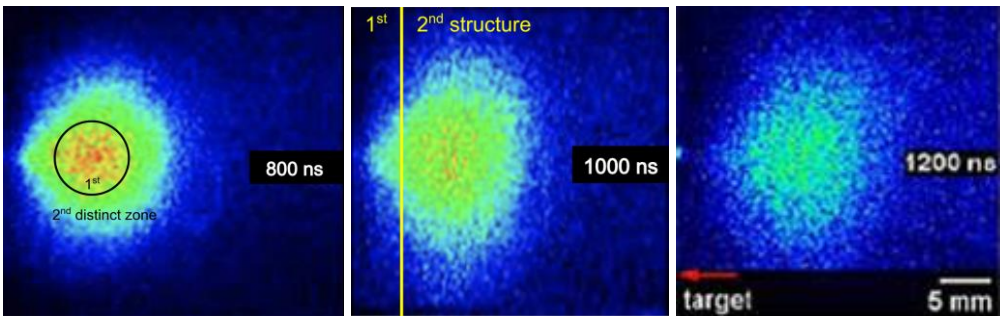

Fig. 6. Two distinct plasmatic structures in polymer plasma plume

The attendance of two obvious maximums in the 2-dimensional pictures was attributed to the two plasma distinct components, differently colored in the images shown. According to the distinction in their expansion rate, by observing two apparent velocities of displacement, in papers of specialty publications, they could be justified as being the rapid plasma frame/composition (namely “first plasma structure”) and sluggish plasma frame (namely “second plasma structure”), respectively. Evidently, both plasma structures extend with constant, but separate velocities values [9].

Regarding the successful experiments undertaken, we mention that 10 plasma feather samples were investigated in order to obtain different behavior in the field of motion, respectively to highlight the presence of the two distinct speeds. The

determinations that led to the realization of the figure, are made for the so-called the sample # 3, from laser produced plume plasmas.

Time delay is 550ns between the two separate plasma plume structures. In addition, the different plasma feather substructures were represented with different colors to distinguish each other. Thus, the first substructure was designated with the color olive, while the second substructure was designated with the color green, Figure 7.

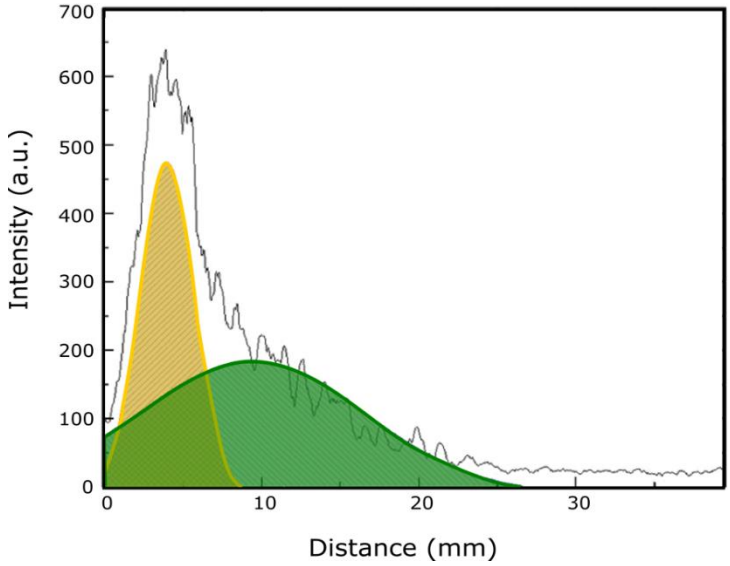

Fig. 7. Two distinct velocities in ICCD snapshot aggregate on 1000 ns period (transversal section perspective)

The velocity calculated of every structure has been conditioned by the ratio of distance and time, for displacement of the maximum loudness specific feature to every plasma plume structure, procedure in conjunction with the physical point of view of the laser, which causes plasma extension at several types of pressure, low and medium, for example [12, 13]. The constant velocities character of the extension process is determined by the natural linearity of physical phenomenon observed, with respect to all examined plasmas, so far.

Conclusions

The laser ablation of the diblock copolymer (PS-b-P4VP) and associated plasma plume behavior are carefully investigated.

From the exploitation of laboratory measurements, the temperature function depending on two variables, time and position, respectively, has been successfully obtained. As associated illustrations, the graphic representations of the complete

solutions for the temperature distribution in two-dimensional and three-dimensional cases are introduced. In the paper, the experimental results of the laser-ablation modification of copolymer films having nano-scale microdomain structures were analyzed. Further, benefiting from the physical correct interpretation, any of the experimental results (e.g., the velocity of plasma structures generated by laser ablation has a constant value) can be explained. All these observations made on the polymeric plasma, achieved by means of laser ablation, completed the complex particular image of the phenomenon discussed here. Additionally, a favorable correlation between the experimental data obtained by authors with those known from the specialized literature was highlighted.

R E F E R E N C E S

[1] R. J. Goldsten and P.H. Rutherford, *Introduction to Plasma Physics* (CRC Press, Bristol, 1995).

[2] R. Srinivasan, V. Mayne-Banton, Appl. Phys. Lett. **41**, 576 (1982).

[3] M. R. Hauer, Dissertation Paper (ETH Library, Zürich, 2004).

[4] N. Bityurin, B. S. Lukyanchuk, M. H. Hong and T. C. Chong, Chem. Rev.**103**, 519, (2003).

[5] S. Gurlui, M. Agop, P. Nica, M. Ziskind and C. Focsa, Phys. Rev. E **78**: 026405, (2008).

[6] O. Niculescu, D. G. Dimitriu, V. P. Paun, *et al.*, *Physics of Plasmas* **17(4)**: 042305, (2010).

[7] P. D. Ioannou, P. Nica, V. Paun, *et al*., Physica Scripta **78(6)**: 065101, (2008).

[8] N. Cimpoesu, S. Gurlui, G. Bulai, R. Cimpoesu, V.P. Paun, S.A. Irimiciuc and M. Agop, Symmetry **12(1)**, 109, (2020).

[9] M. A. Paun, V. A. Paun and V. P. Paun, Entropy **24(3)**, 342, (2022).

[10] O. C. Zienkiewicz, R. L. Taylor and J. Z. Zhu, *The Finite Element Method: Its Basis and Fundamentals*; (Butterworth-Heinemann, Oxford, UK 2005).

[11] J. Fish and T. Belytschko, *A First Course in Finite Elements*, (John Wiley & Sons Ltd., Chichester, West Sussex PO19 8SQ, UK 2007).

[12] J. J. Camacho, M. Oujja, M. Sanz, *et al.*, J. Anal. At. Spectrom. **34(2)**, (2019).

[13] S. Ravi-Kumara, B. Liesa, H. Lyub and H. Qina, Procedia Manufacturing **34,** 316, (2019).